Definition of the hypothalamic GnRH pulse generator in mice

Jenny Clarkson[a,b,1], Su Young Han[a,b,1], Richard Piet[a,b], Timothy McLennan[a,b], Grace M. Kane[a,b], Jamie Ng[a,b], Robert W. Porteous[a,b], Joon S. Kim[a,b], William H. Colledge[c], Karl J. Iremonger[a,b], and Allan E. Herbison[a,b,2]

[a]Centre for Neuroendocrinology, University of Otago, Dunedin 9054, New Zealand; [b]Department of Physiology, School of Biomedical Sciences, University of Otago, Dunedin 9054, New Zealand; and [c]Reproductive Physiology Group, Department of Physiology, Development and Neuroscience, University of Cambridge, Cambridge CB2 3EG, United Kingdom

Edited by Joseph S. Takahashi, Howard Hughes Medical Institute, University of Texas Southwestern Medical Center, Dallas, TX, and approved October 13, 2017 (received for review August 6, 2017)

The pulsatile release of luteinizing hormone (LH) is critical for mammalian fertility. However, despite several decades of investigation, the identity of the neuronal network generating pulsatile reproductive hormone secretion remains unproven. We use here a variety of optogenetic approaches in freely behaving mice to evaluate the role of the arcuate nucleus kisspeptin (ARN^{KISS}) neurons in LH pulse generation. Using GCaMP6 fiber photometry, we find that the ARN^{KISS} neuron population exhibits brief (∼1 min) synchronized episodes of calcium activity occurring as frequently as every 9 min in gonadectomized mice. These ARN^{KISS} population events were found to be near-perfectly correlated with pulsatile LH secretion. The selective optogenetic activation of ARN^{KISS} neurons for 1 min generated pulses of LH in freely behaving mice, whereas inhibition with archaerhodopsin for 30 min suppressed LH pulsatility. Experiments aimed at resetting the activity of the ARN^{KISS} neuron population with halorhodopsin were found to reset ongoing LH pulsatility. These observations indicate the ARN^{KISS} neurons as the long-elusive hypothalamic pulse generator driving fertility.

fertility | GnRH | kisspeptin | pulse | arcuate nucleus

Endocrine signaling from the pituitary gland occurs primarily as pulsatile hormone secretion. For most hormones, this pulsatility is thought to be generated by episode generators located within the hypothalamus and pituitary gland (1, 2). However, with few exceptions, it has been extremely difficult to determine the identity and nature of these neuroendocrine pulse generators (3, 4). Although the importance of pulsatile hormone secretion for reproduction was discovered in the 1970s (5, 6), the identity of the so-called gonadotropin-releasing hormone (GnRH) pulse generator (7, 8) responsible for pulsatile gonadotropin secretion remains unknown.

The discovery of the critical importance of kisspeptin signaling within the brain of humans and rodents for fertility (9–11) has suggested a potential role for kisspeptin signaling in the generation of pulsatile hormone secretion. Humans and rodents with global deletions or mutations in kisspeptin or the kisspeptin receptor fail to exhibit normal pulsatile luteinizing hormone (LH) secretion (9, 10, 12, 13). Of the two kisspeptin neuron populations that innervate GnRH neurons, particular attention has focused upon the arcuate nucleus kisspeptin (ARN^{KISS}) neurons in terms of pulse generation (14, 15). Investigators have shown that ARN^{KISS} neurons coexpress a variety of different neurotransmitters, including glutamate, neurokinin B, and dynorphin (15, 16), for which these cells also express functional receptors (17, 18). Alongside anatomical evidence, it has been suggested that the ARN^{KISS} neurons may exhibit synchronized behavior that could intermittently activate GnRH neurons and, thus, act as a pulse generator (15, 16, 19). This attractive hypothesis remains unproven.

We employ here a range of optogenetic approaches in freely behaving mice to evaluate whether the ARN^{KISS} neurons represent the GnRH pulse generator. Using GCaMP fiber photometry, we observed brief repetitive episodes of elevated calcium within the ARN^{KISS} neuron population and found a near-perfect correlation of these events with pulsatile LH secretion. Mimicking these brief synchronization events through selective channelrhodopsin (ChR2) activation of ARN^{KISS} neurons was sufficient to generate pulsatile LH secretion, while optogenetic inhibition of ARN^{KISS} neurons suppressed pulsatile LH secretion. Further, resetting the activity of the ARN^{KISS} neuron population was found to reset pulsatile LH secretion. Together, these observations indicate that the ARN^{KISS} neurons are the GnRH pulse generator.

Results

ARN^{KISS} Neurons Exhibit Episodic Activity in Vivo. We used fiber photometry (20) to examine whether ARN^{KISS} neurons exhibited intermittent synchronous activity in awake freely behaving mice. We targeted the calcium reporter GCaMP6s to ARN^{KISS} neurons by bilateral injection of AAV9-CAG-Flex-GCaMP6s into the ARN of male KISS1-Cre;tdTomato reporter mice (21). Immunohistochemical analyses showed that GCaMP6 was expressed in kisspeptin neurons throughout the ARN, with 51 to 67% of ARN^{KISS} neurons expressing GCaMP6 depending on rostrocaudal level (Fig. S1). Dual-labeled cells represented 89 ± 6 to 96 ± 6% of all GCaMP6-expressing cells in the ARN (Fig. S1). Acute brain slice experiments using cell-attached recording combined with GCaMP6 calcium imaging showed that GCaMP6 faithfully reports on the electrical activity of ARN^{KISS} neurons in these mice (six cells from four mice; Fig. 1*B*).

Significance

Neural networks located in the hypothalamus are responsible for generating ultradian patterns of hormone secretion that control a wide variety of functions. How these neural networks generate pulsatile hormone secretion remains unknown. We report here that a population of hypothalamic kisspeptin neurons represents the gonadotropin-releasing hormone (GnRH) pulse generator. These cells have the remarkable ability to generate synchronized GnRH secretion every 9 min to drive pulsatile gonadotropin hormone secretion in the blood. These observations indicate the arcuate kisspeptin neurons as the origin of reproductive hormone pulsatility in mice and offer the prospect of better understanding and manipulating fertility in the clinic.

Author contributions: J.C., S.Y.H., R.P., and A.E.H. designed research; J.C., S.Y.H., R.P., T.M., G.M.K., J.N., and R.W.P. performed research; J.S.K., W.H.C., and K.J.I. contributed new reagents/analytic tools; J.C., S.Y.H., R.P., K.J.I., and A.E.H. analyzed data; and J.C., S.Y.H., R.P., K.J.I., and A.E.H. wrote the paper.

The authors declare no conflict of interest.

This article is a PNAS Direct Submission.

[1]J.C. and S.Y.H. contributed equally to this work.

[2]To whom correspondence should be addressed. Email: allan.herbison@otago.ac.nz.

This article contains supporting information online at www.pnas.org/lookup/suppl/doi:10.1073/pnas.1713897114/-/DCSupplemental.

We next injected a group of KISS1-Cre male mice with GCaMP6 AAV (adeno-associated virus) and implanted a 400-μm-diameter optical fiber just above the ARN (Fig. 1*A*). Mice were gonadectomized (GDX) to generate a state in which the GnRH pulse generator is operating at its highest frequency. After 3 wk of daily handling and habituation, the mice were connected to the patch cord of a fiber photometry system and calcium signals were measured for up to 4 h in freely behaving mice. Abrupt increases in calcium signal were detected at approximately regular intervals of 8.9 ± 0.5 min (range, 4.5 to 20.7 min) in all mice examined ($n = 7$; Fig. 1*C*). Histological analysis showed that all optical fibers were located above the middle to caudal aspect of the ARN. High-frequency photometry sampling revealed a consistent temporal dynamic for calcium events, with an initial rapid increase over 19.6 ± 2.4 s followed by a slower decrease that, together, lasted for 74.2 ± 6.6 s (16 events from 7 mice; Fig. 1 *D* and *E*).

To demonstrate that the GCaMP6 signal reflects the activity of ARN^{KISS} neurons, we coinjected Cre-dependent AAVs for both GCaMP6s and hM3Dq (22) into the ARN of GDX KISS1-Cre mice. Three to 4 wk later, calcium imaging experiments in acute brain slices demonstrated that addition of 1 to 10 μM clozapine *N*-oxide (CNO) to the bathing medium resulted in a marked and prolonged increase in both firing and intracellular calcium concentrations ($[Ca^{2+}]i$) in all ARN^{KISS} neurons (4 cells dual-recorded, 38 cells in total, three mice; Fig. 1*F*). KISS1-Cre mice injected with GCaMP6s and hM3Dq were then prepared with a photometry fiber directed at the ARN. Peripheral administration of CNO (i.p., 2 mg/kg) to freely behaving mice was found to rapidly (within 5 min) enhance basal $[Ca^{2+}]i$ by 33 ± 8% and increase the frequency of calcium events by 100 ± 52% ($P = 0.04$, paired t test; $n = 4$; Fig. 1*G*).

These studies indicate that ARN^{KISS} neurons exhibit episodes of synchronized activity every ∼9 min. This was surprising, as previous estimates of GnRH pulse generator activity in GDX mice, obtained from measuring plasma LH levels (23), indicated a GnRH/LH pulse interval of >20 min. We next examined the

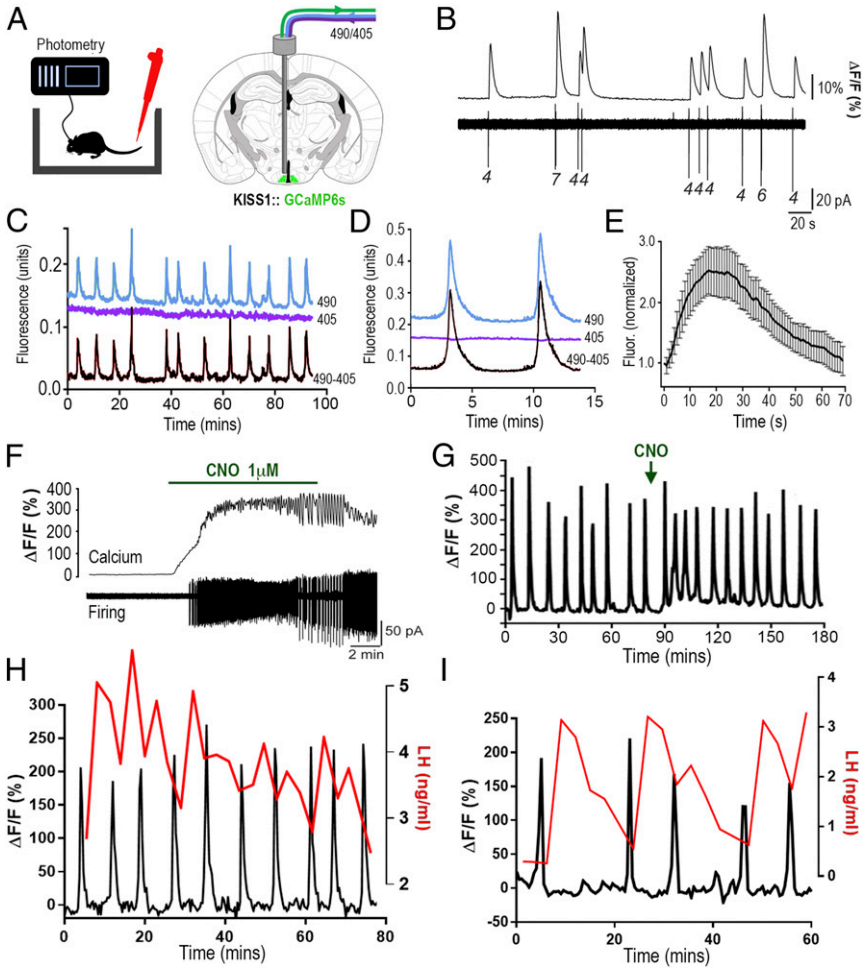

Fig. 1. ARN^{KISS} neurons exhibit periodic synchronizations in intracellular calcium concentrations tightly correlated with pulsatile LH secretion in gonadectomized male mice. (*A*) KISS1-Cre mice injected with Cre-dependent GCaMP6s AAV into the ARN (green) and connected to a fiber photometry system with regular blood sampling from the tail tip. Alternating 490-nm (Ca^{2+}-dependent) and 405-nm (Ca^{2+}-independent) wavelength light passes down the photometry fiber. (*B*) Simultaneous GCaMP6s calcium (*Top*) and cell-attached (*Bottom*) recordings from an ARN^{KISS} neuron. Numbers indicate spikes per burst. (*C*) Fluorescence emission traces (490-nm calcium, blue; 405-nm background, purple) recorded from ARN^{KISS} neurons of a gonadectomized male mouse with the subtracted signal (490 − 405) shown below. (*D*) Continuous recording of two calcium events from a gonadectomized mouse. (*E*) Average fluorescence waveform of calcium events (16 events, 7 mice) normalized to the beginning of each event. (*F*) Simultaneous brain slice recording of GCaMP6s fluorescence (*Top*) and action potential firing (*Bottom*) from a GCaMP6s/hM3Dq-expressing ARN^{KISS} neuron showing the response to CNO applied in the bath. (*G*) Representative trace showing the effect of i.p. CNO (arrow) on GCaMP6 calcium signal from ARN^{KISS} neurons in a gonadectomized mouse. (*H* and *I*) Representative dual calcium and plasma LH traces showing the near-perfect correlation of ARN^{KISS} neuron GCaMP6 calcium events (black) with pulses of LH secretion (red) in two separate gonadectomized male mice. (*I*) The mouse with the slowest calcium events is shown.

relationship of ARN^{KISS} neuron calcium events to pulsatile LH secretion by taking 3-min tail-tip blood samples for a 60- to 80-min period while also monitoring calcium signals. This revealed that calcium events were almost perfectly correlated with increments in LH secretion; 94% of calcium events were followed by a >10% increase in LH concentration. No increases in LH were detected without a preceding calcium event (60 LH pulses in seven mice; Fig. 1 *H* and *I*). The interval from the peak of the calcium event to the peak of the LH pulse was highly consistent across all animals, being 4.00 ± 0.14 min ($n = 7$). A significant temporal relationship existed between calcium and LH peaks ($P < 0.05$, repeated-measures ANOVA), while no such relationship existed between randomly selected LH samples and calcium peaks (Fig. S2).

Brief Activation of ARN^{KISS} Neurons Generates LH Pulses in Vivo. We have previously demonstrated that optogenetic activation of ARN^{KISS} neurons for >2 min at 10 Hz generates pulse-like increments in LH secretion in anesthetized mice (24). However, the fiber photometry studies above clearly demonstrate that ARN^{KISS} neuron calcium events last for only ∼1 min. Hence, we examined whether brief 1-min periods of ARN^{KISS} neuron activation were sufficient to evoke an LH pulse in awake freely behaving mice.

Channelrhodopsin was targeted to ARN^{KISS} neurons by unilateral injection of AAV9-EF1-dflox-hChR2-mCherry into the ARN of intact male and female KISS1-Cre mice (24). Intact mice exhibited an LH pulse every 90 to 180 min (12, 23), thereby providing a long window of basal LH secretion for optogenetic stimulation experiments. Activation of ARN^{KISS} neurons for 1 min (10 Hz, 473-nm light, 5 mW) was found to reliably evoke pulse-like increments in LH secretion in conscious male ($n = 5$; Fig. 2 *A*–*C*) and female ($n = 6$; Fig. 2 *D* and *E*) mice, and this was repeatable at 30-min intervals. Compatible with sex differences in endogenous LH pulse amplitude (12, 23), optogenetic activation of ARN^{KISS} neurons evoked 0.5- to 1-ng/mL amplitude LH pulses in females (Fig. 2 *D* and *E*) and ∼4-ng/mL amplitude pulses in males (Fig. 2 *B* and *C*). The profile of LH secretion evoked by 10-Hz, 1-min stimulation was very similar to the profile of endogenous LH pulses observed in intact male mice (Fig. 2*F*).

The Inhibition of ARN^{KISS} Neuron Firing Suppresses Pulsatile LH Secretion in Vivo. To examine the necessity of ARN^{KISS} neurons for pulsatile LH secretion, we employed an optogenetic archaerhodopsin (ArchT)-mediated silencing approach (25, 26). Bilateral injections of a Cre-dependent ArchT-tdTomato AAV were made into the ARN of adult female KISS1-Cre;GFP reporter mice that were also GDX at the time of surgery to generate high-frequency pulsatile LH secretion. This resulted in 60 to 69% of ARN^{KISS} neurons expressing ArchT (Fig. 3*B* and Fig. S3), representing 77 to 83% of all ArchT-expressing neurons depending on rostrocaudal location within the ARN (Fig. S3). The use of a GFP reporter for labeling kisspeptin neurons is not as efficient as the tdTomato reporter [GCaMP6 and eNpHR3.0 (halorhodopsin) experiments] and, consequently, underreports the number of ARN^{KISS} neurons (Figs. S1, S3, and S4).

Cell-attached recordings from ARN^{KISS} neurons in acute brain slices prepared from ArchT AAV-injected KISS1-Cre mice demonstrated that 532-nm green light promptly suppressed firing rates by 76 ± 8% over the 5-min period, with a gradual return to baseline firing when illumination was stopped (11 cells from 5 mice; Fig. 3 *C* and *D*). As ARN^{KISS} neurons exhibit very low levels of spontaneous electrical activity in the brain slice, 10 to 20 nM neurokinin B (NKB) was added to the bathing medium to increase their firing (27).

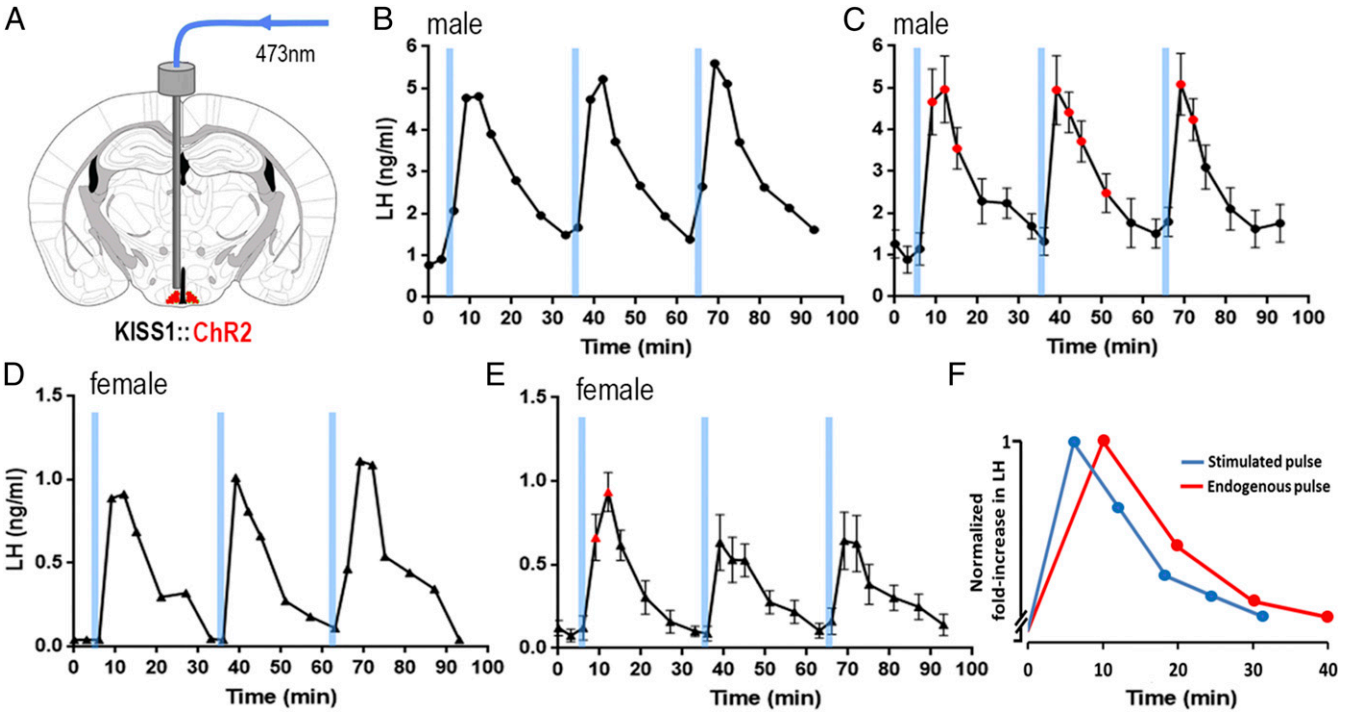

Fig. 2. Brief 1-min channelrhodopsin activation of ARN^{KISS} neurons evokes pulsatile LH secretion in freely behaving intact male and female mice. (*A*) Schematic of experiment. (*B*) Repeated 1-min blue light (473-nm) activations of ARN^{KISS} neurons evoke LH pulses in an intact male mouse. (*C*) Mean (±SEM) LH levels (red symbols indicate significantly elevated LH levels; repeated-measures ANOVA with Dunnett's post hoc tests; $n = 5$). (*D*) Repeated 1-min blue light (473-nm) activations of ARN^{KISS} neurons evoke LH pulses in an intact female mouse. (*E*) Mean (±SEM) LH levels (red symbols indicate significantly elevated LH levels; repeated-measures ANOVA with Dunnett's post hoc tests; $n = 6$). (*F*) Overlaid profiles of endogenous (red) and ChR2-activated (blue) LH pulses in intact male mice. Pulses are normalized for fold increase over baseline; endogenous LH pulses ($n = 6$) were sampled every 10 min and ChR2-activated LH pulses ($n = 15$) every 6 min.

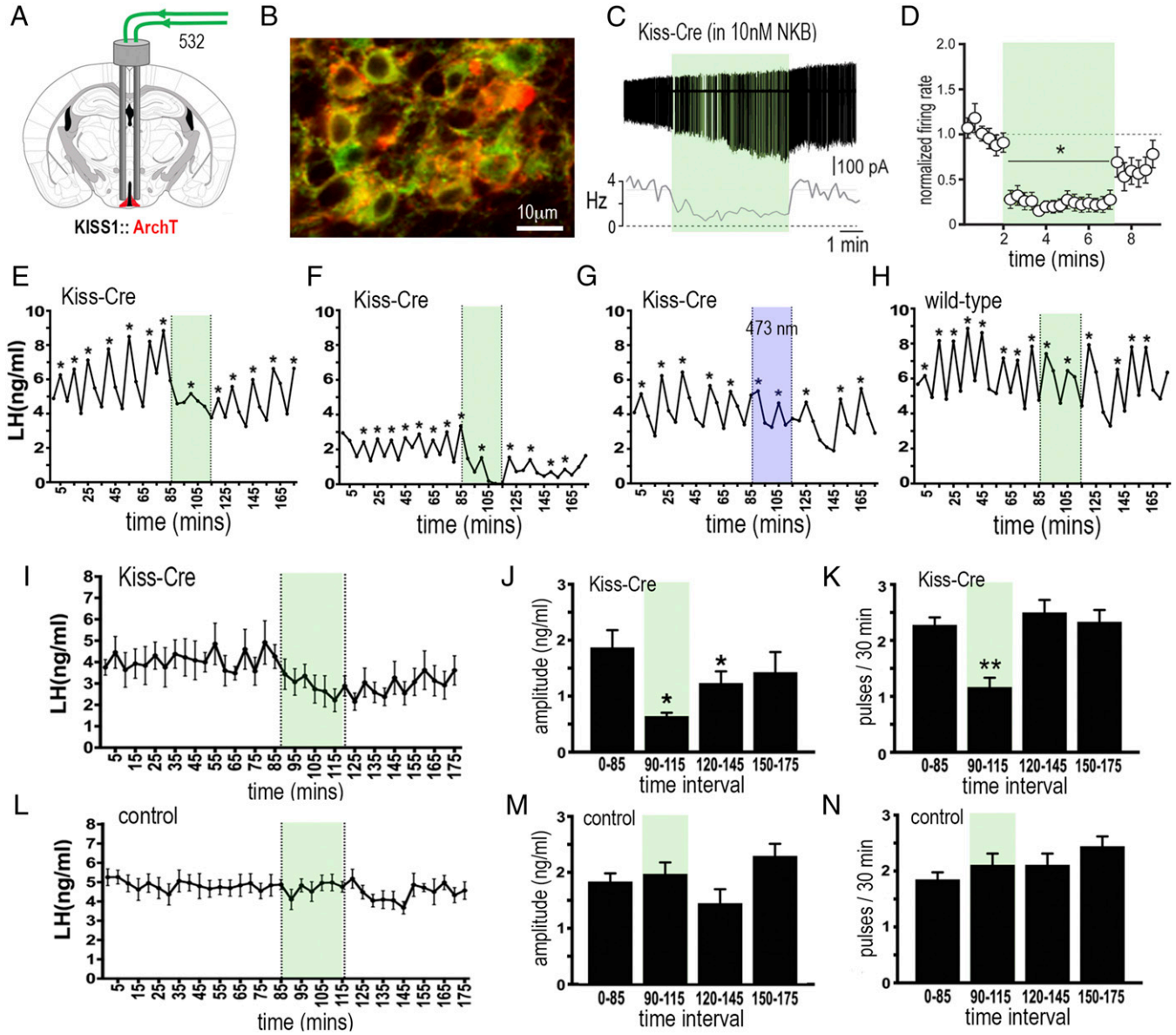

Fig. 3. Archaerhodopsin inhibition of ARN^{KISS} neurons suppresses pulsatile LH secretion in gonadectomized female mice. (*A*) KISS1-Cre mice injected with Cre-dependent ArchT-tdTomato AAV into the ARN (red) and implanted with bilateral optic fibers in the ARN. (*B*) Dual fluorescence image of ARN^{KISS} neurons expressing ArchT (red) and kisspeptin (GFP reporter). (*C*) Action potential firing in an ArchT-expressing ARN^{KISS} neuron in the presence of 10 nM NKB in a brain slice. The neuron responds to green light illumination (shading) with a decrease in firing followed by a return to control levels. (*C*, *Top*) Action potential firing. (*C*, *Bottom*) Rate meter for the same cell. (*D*) Mean (±SEM) normalized firing rate of ARN^{KISS} neurons ($n = 11$) responding to green light. *$P < 0.05$ compared with baseline, Friedman test. (*E–H*) Pulsatile LH secretion in ArchT KISS1-Cre (*E–G*) and wild-type (*H*) gonadectomized female mice. Green light illumination (30 min) is indicated by green shading; LH pulses are indicated by asterisks. The trace in *G* shows the same mouse as in *F* but illuminated with blue light. (*I*) Mean (±SEM) LH levels in KISS1-Cre mice ($n = 6$) showing the suppression of LH secretion during green light illumination and subsequent slow recovery. (*J* and *K*) Mean (±SEM) LH pulse amplitude and pulse frequency before (0 to 85 min), during (90 to 115 min; green shading), and subsequent to (120 to 145 and 150 to 175 min) green laser illumination. *$P < 0.05$, **$P < 0.01$ versus 0 to 85 min, ANOVA with Dunnett's post hoc tests; $n = 6$. (*L–N*) Basal (±SEM) LH levels and LH pulse amplitude and frequency in control mice including blue light-illuminated KISS1-Cre and wild-type AAV-injected mice ($n = 8$).

In awake mice ($n = 6$), bilateral green light activation of ArchT in ARN^{KISS} neurons for a 30-min period resulted in a 49% suppression of LH pulse frequency ($P < 0.01$; repeated-measures ANOVA with post hoc Dunnett's tests), 65% decrease in the amplitude of pulses occurring during illumination ($P < 0.05$; repeated measures ANOVA with post hoc Dunnett's tests), and 49% decline in basal LH secretion (Fig. 3 *E*, *F*, and *I–K*). Controls ($n = 9$) included blue light illumination in four mice previously showing LH pulse inhibition with green light (Fig. 3*G*), and green light illumination of wild-type mice injected with the Cre-dependent ArchT AAV (Fig. 3*H*) and Kiss-Cre mice without ArchT. In all cases, laser illumination had no effect on LH secretion (Fig. 3 *L–N*).

Resetting the Activity of ARC^{KISS} Neurons Resets Pulsatile LH Secretion in Vivo. The above studies show that ARC^{KISS} neuron activity is both necessary and sufficient for pulsatile LH secretion in the mouse. However, it remains possible that these cells represent a relay of the pulse generator rather than being the episode generator themselves. In the course of developing the optogenetic methodology for this study, we also examined halorhodopsin as a potential inhibitory tool. Electrophysiological studies on eNpHR3.0-expressing

ARC^{KISS} neurons revealed that 532-nm green light evoked a mean 81 ± 4% inhibition, and often complete silencing, of NKB-activated ARC^{KISS} neurons but then resulted in a marked rebound activation for up to 2 min when illumination was stopped (Fig. 4 *C* and *D*). This represented an ideal way to temporally reset the activity of the ARC^{KISS} neuron population in vivo. As such, we undertook a second series of optogenetic inhibition studies using eNpHR3.0 to both confirm the ArchT result and also determine whether we could reset LH pulsatility through manipulation of only the ARN^{KISS} neurons.

Bilateral injections of Cre-dependent eNpHR3.0 AAV were made into the ARN of adult GDX female KISS1-Cre mice. This

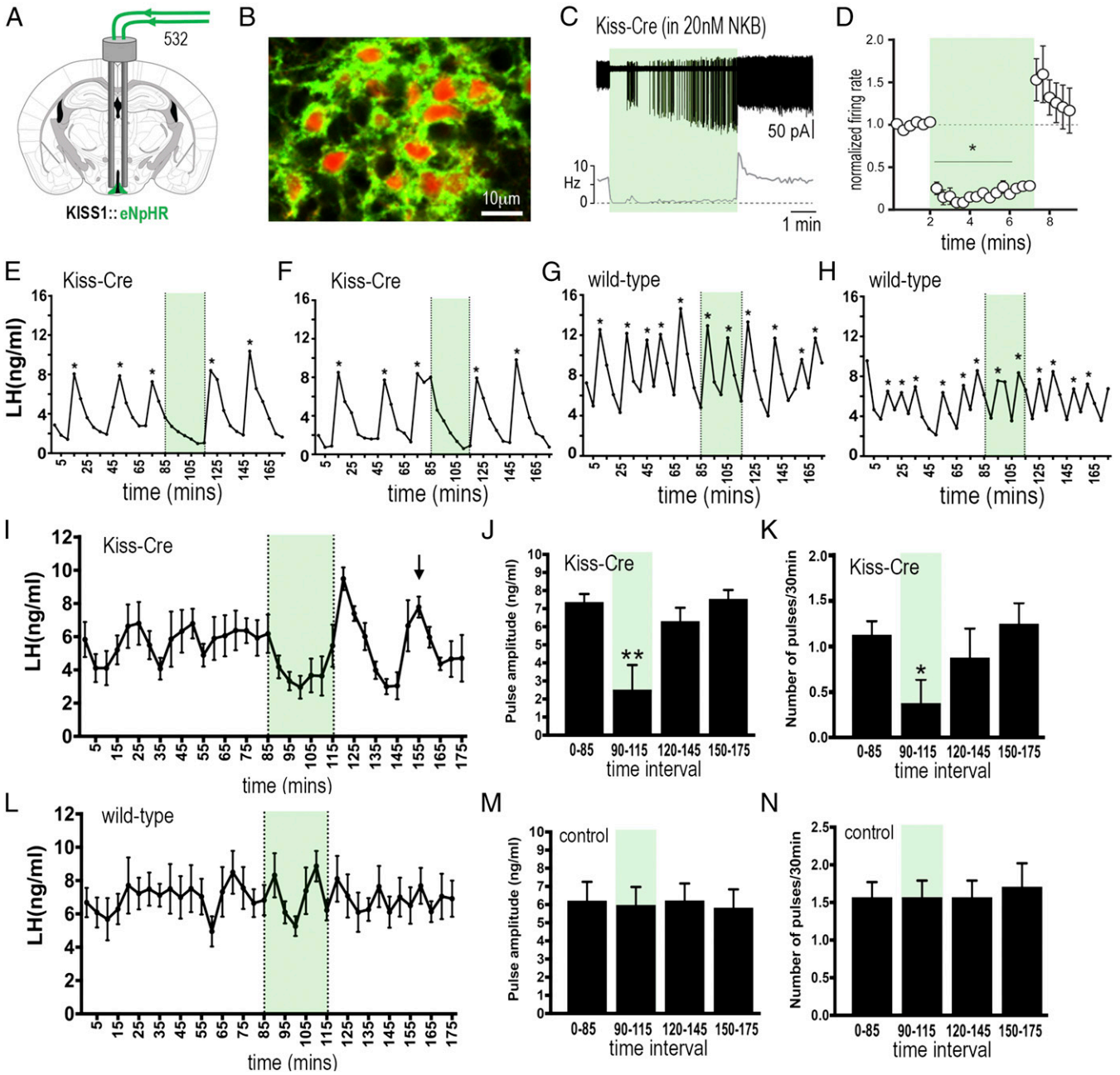

Fig. 4. Halorhodopsin inhibition and activation of ARN^{KISS} neurons suppresses and then initiates ongoing pulsatile LH secretion in gonadectomized female mice. (*A*) KISS1-Cre mice injected with Cre-dependent eNpHR3.0-eYFP AAV into the ARN (green) and implanted with bilateral optic fibers in the ARN. (*B*) Dual fluorescence image of ARN^{KISS} neurons expressing eNpHR3.0 (green) and kisspeptin (tdTomato reporter). (*C*) Action potential firing in an eNpHR3.0-expressing ARN^{KISS} neuron in the presence of 20 nM NKB. The neuron responds to green light with an abrupt decrease in firing followed by a sharp rebound activation immediately after the light is stopped. (*C*, *Top*) Action potential firing. (*C*, *Bottom*) Rate meter. (*D*) Mean (±SEM) normalized firing rate of ARN^{KISS} neurons ($n = 6$) responding to green light. *$P < 0.05$ compared with baseline, Friedman test. (*E–H*) Pulsatile LH secretion in eNpHR3.0 KISS1-Cre (*E* and *F*) and wild-type (*G* and *H*) gonadectomized female mice. Green light illumination is indicated by green shading and LH pulses are indicated by asterisks. (*I*) Mean (±SEM) LH levels in KISS1-Cre mice ($n = 8$) showing the suppression of LH secretion during green light illumination and the subsequent rebound of LH and resetting of the pulse generator to evoke a subsequent LH pulse in all mice (arrow). (*J* and *K*) Mean (±SEM) LH pulse amplitude and pulse frequency before (0 to 85 min), during (90 to 115 min; green shading), and subsequent to (120 to 145 and 150 to 175 min) green laser illumination. *$P < 0.05$, **$P < 0.01$ versus 0 to 85 min, ANOVA with post hoc Dunnett's test; $n = 8$. (*L–N*) Basal (±SEM) LH levels and LH pulse amplitude and frequency in control AAV-injected wild-type mice ($n = 7$).

resulted in 63 to 70% of ARC^{KISS} neurons expressing eNpHR3.0 (Fig. 4*B* and Fig. S4), with dual-labeled neurons accounting for up to 94% of all eNpHR3.0 cells depending on rostrocaudal location within the ARN (Fig. S3).

Bilateral green light activation of eNpHR3.0 in ARC^{KISS} neurons resulted in the suppression of pulsatile LH secretion for the 30-min duration of illumination (Fig. 4 *E* and *F*; $n = 8$). This resulted in a 66% decrease in LH pulse frequency ($P < 0.05$, ANOVA with post hoc Dunnett's tests), with five of eight mice exhibiting a complete suppression of pulsatile LH release during the 30-min illumination period (Fig. 4 *E* and *F*). The remaining three mice exhibited a single pulse during this time with, overall, a 65% reduction in LH pulse amplitude ($P < 0.01$, ANOVA with post hoc Dunnett's tests; Fig. 4*J*). Control mice ($n = 7$), including wild-type mice injected with eNpHR3.0 AAV and KISS1-Cre mice with off-target fiber optic placements, did not exhibit any changes in pulsatile or basal LH secretion during green light illumination (Fig. 4 *G*, *H*, and *L*–*N*). Four mice with unilateral activation of eNpHR3.0 in ARN^{KISS} neurons did not exhibit any changes in LH (Fig. S5*E*).

As predicted, a robust LH pulse was generated immediately after termination of the green light illumination in eNpHR3.0 KISS1-Cre mice (Fig. 4 *E*, *F*, and *I*), but not in controls (Fig. 4 *G*, *H*, and *L*). KISS1-Cre mice also exhibited a resetting of ongoing LH pulsatility (Fig. 4 *E* and *F*). As observed with mean LH values (Fig. 4*I*), the random timing of LH pulses in individual mice results in an averaged flat line before a fall in mean LH levels upon illumination and the initiation of an LH pulse when the laser is turned off. Subsequent to this evoked pulse, another pulse was found to occur 35 min later in all mice (Fig. 4*I*, arrow). Control mice, and indeed ArchT KISS1-Cre mice (Fig. 3*I*), do not show any relationship between LH pulsatility and green light termination (Fig. 4 *G*, *H*, and *L*). For unknown reasons, the expression of eNpHR3.0 in ARC^{KISS} neurons generates mice with large, relatively slow LH pulses independent of any illumination. As such, LH pulses occur every 34 min in these mice (Fig. 4*K*), and this was consistent with the ongoing 35-min pulse interval found after resetting LH pulse frequency with eNpHR3.0 (Fig. 4*I*).

In undertaking the eNpHR3.0 experiments, we generated cohorts of KISS1-Cre mice in which eNpHR3.0 was expressed throughout the ARN but optical fibers were located bilaterally in either the rostral ($n = 5$) or middle/caudal ($n = 7$) ARN (Fig. S5). Whereas bilateral light activation of the middle/caudal ARN^{KISS} neurons was always effective in suppressing pulsatile LH secretion, illumination of the rostral ARN^{KISS} had no (Fig. S5*F*), or only partial (Fig. S5*G*), effects on pulsatile LH secretion.

Discussion

We demonstrate here that ARN^{KISS} neurons are almost certainly the long-elusive hypothalamic GnRH pulse generator. These neurons exhibit episodes of synchronized activity lasting ∼1 min that are almost perfectly correlated with pulsatile LH secretion. Consistent with this, the activation of ARN^{KISS} neurons for 1 min reliably generated pulses of LH secretion. Using two inhibitory optogenetic strategies, we show that the selective inhibition of ARN^{KISS} neuron activity results in the suppression of pulsatile LH secretion. Furthermore, the resetting of ARN^{KISS} neuron activity is found to reset pulsatile LH secretion.

The calcium events detected with fiber photometry very likely represent the synchronized electrical activity of the ARN^{KISS} neurons. In brain slice experiments, we found that GCaMP6 reliably reported ARN^{KISS} neuron firing. Furthermore, coexpression of GCaMP6 and hM3Dq in ARN^{KISS} neurons demonstrated that the CNO-induced activation of firing in ARN^{KISS} neurons was associated with large increases in $[Ca^{2+}]i$ within individual ARN^{KISS} neurons. We noted that, in vivo, CNO raised the basal calcium signal and doubled the frequency of synchronized calcium events. This shows that the ARN^{KISS} neuron population can maintain an episodic synchronized output in the presence of persistent Gq protein-coupled receptor activation. This did not occur in the acute brain slice, where CNO evoked a long-lasting activation of both firing and $[Ca^{2+}]i$ in individual ARN^{KISS} neurons with no evidence of episodic activity. This possibly results from the absence of network activity in the acute brain slice, where the deafferentated ARN^{KISS} neurons show little spontaneous activity and no episodic or synchronous firing (18, 27).

The ARN^{KISS} neuron population exhibits robust increases in calcium approximately every 9 min. This was unexpected, given that prior assessments of pulse generator activity had indicated the LH pulse interval to be >20 min (28). Nevertheless, we find here that 94% of synchronized calcium events are followed by an increment in LH secretion in gonadectomized mice. Often these changes in LH did not occur as a classical pulse but could be observed, for example, as an increment in LH on the downward shoulder of a prior LH pulse. These events are not detected by current pulse analysis algorithms, and indicate the need for the further development of LH pulse analysis methodologies. In terms of ARN function, it is intriguing to find a 10-min neuronal oscillator embedded among ARN neural circuitries subserving longer-term functions such as feeding initiation (29). With evidence for kisspeptin inputs into these feeding circuits and others (30), it will be interesting to examine the impact of this fast oscillator on other ARN outputs in future studies.

The selective inhibition of ARN^{KISS} neuron activity with both ArchT and eNpHR3.0 optogenetic strategies suppressed pulsatile LH secretion. We found that the eNpHR3.0 approach generated a stronger inhibition of ARN^{KISS} neuron firing in vitro and that this correlated with a more robust inhibition of LH pulsatility compared with ArchT. It is likely that a subpopulation of the ∼1,000 ARN^{KISS} neurons in the mouse (21) is required for pulse generation. Only ∼70% of ARN^{KISS} neurons expressed ArchT or eNpHR3.0 in our experiments, and fiber optic locations in the rostral ARN were ineffective in suppressing pulsatile LH secretion. This raises the possibility that a subpopulation of kisspeptin neurons located in the midcaudal ARN may comprise the GnRH pulse generator. How few ARN^{KISS} neurons may be required for pulsatility is not known, but a 30% suppression of total *Kiss1* mRNA expression in the ARN does not appreciably alter LH pulsatility in rats (31). Unilateral suppression of ARN^{KISS} neuron activity was insufficient to alter LH pulsatility, whereas unilateral activation generated LH pulses. Contralateral projections between the bilateral ARN^{KISS} neuron networks may maintain their synchronization (18, 32), although activation of a unilateral population is sufficient to generate an LH pulse.

Although the ChR2 and ArchT optogenetic studies demonstrated the necessity and sufficiency of ARN kisspeptin neurons for pulse generation, they did not establish whether this population was, itself, the pulse generator. The silencing followed by rebound activation of ARN^{KISS} after eNpHR3.0 activation provided a useful tool to explore this issue. Rebound activation has been reported following eNpHR, but not ArchT, activation in other neural populations, and may result from chloride ion-based changes in $GABA_A$ reversal potential (33). We predicted that if ARC^{KISS} neurons were simply a relay within the pulse generator, then eNpHR3.0-mediated synchronous activation would have no impact upon LH pulsatility beyond the initiated pulse. On the other hand, if the ARC^{KISS} neurons were the genesis of pulsatility, this randomly timed activation should be able to reset future pulsatile LH secretion. This was indeed found to be the case, with synchronous eNpHR3.0 activation generating an LH pulse upon offset as well as a subsequent time-locked spontaneous LH pulse ∼35 min later in every mouse. This occurred regardless of when the stimulus was applied in relation to endogenous LH pulsatility. We were surprised to find that the expression of eNpHR3.0 in ARN^{KISS} neurons resulted in the slowing of LH pulse frequency to ∼34 min independent of any light activation. Light-independent

effects of eNpHR3.0 on neuronal behavior have not been reported previously but, nevertheless, suggest the possibility that changes in ARN^{KISS} neuron chloride ion homeostasis may be one strategy for slowing pulse generator frequency.

Tracing studies in mice have demonstrated that ARN^{KISS} neurons only project to the distal projections of GnRH neurons in the vicinity of the median eminence (34). These distal GnRH neuron projections, termed dendrons, are unusual in that they display both dendrite- and axon-like properties and are regulated directly by multiple neural inputs (35, 36). We show here that ARN^{KISS} neurons likely release kisspeptin for ~1 min to generate an LH pulse. Recent studies have shown that brief (10- to 60-s) applications of kisspeptin to the median eminence increase intracellular calcium levels in GnRH neuron dendrons and evoke GnRH secretion independent of action potential firing in GnRH neurons (36, 37). This ARN^{KISS}→GnRH neuron dendron pathway is also likely to exist in primates, as the closest associations between kisspeptin and GnRH fibers occur in the internal zone of the median eminence of the monkey (38), and kisspeptin levels within the ARN/median eminence fluctuate and can occur coincident with episodes of pulsatile GnRH secretion in this species (39). The ability of ARN^{KISS} neurons to target the merged distal projections of GnRH neurons around the median eminence abrogates the need for a pulse generator to project to the widely dispersed GnRH neuron cell bodies. This represents an atypical mechanism for rhythm generation in the brain (40), and emphasizes the diversity of mechanisms that the neuroendocrine hypothalamo–pituitary axes likely employ to drive the pulsatile hormone secretion.

In conclusion, we provide here robust evidence for the identity of the GnRH pulse generator proposed over three decades ago. It remains that the mechanisms responsible for the synchronization of ARN^{KISS} neurons are unknown. Similarly, it is unclear how gonadal steroids and neuronal inputs proposed to mediate multiple different homeostatic and external influences upon pulsatility (14) interact with ARN^{KISS} neurons. It is expected that the further elucidation of both the intra- and intercellular mechanics of the ARN^{KISS} pulse generator will provide a robust framework for advancing strategies aimed at regulating LH pulse frequency in the clinic.

Methods

Animals. Adult littermate heterozygous KISS1-$Cre^{+/-}$ or KISS1-$Cre^{-/-}$ (21) mice, alone or crossed onto Cre-dependent reporter ROSA26-CAG-τGFP or Ai9-CAG-tdTomato lines (mixed 129S6Sv/Ev C57BL6 genetic background), were housed under a 12:12 h lighting schedule (lights on at 6:00 AM) with ad libitum access to food and water. All experiments were approved by the University of Otago Animal Welfare and Ethics Committee.

Stereotaxic Injections of AAVs. Recombinant Cre-dependent AAVs encoding GCaMP6s (AAV2/9-CAG-FLEX-GCaMP6s-WPRE-SV40, 1.3×10^{13} mol/mL; University of Pennsylvania), ChR2 [AAV2/9-EF1-DIO-hChR2-(H134R)-mCherry-hGH, 5.8×10^{13}; University of Pennsylvania], ArchT (AAV2/9-CAG-FLEX-ArchT-tdTom, 1.5×10^{13}; University of North Carolina), eNpHR3.0 (AAV2/1-EF1-DIO-eNpHR3.0-EYFP, 2.8×10^{13}; University of Pennsylvania), or hM3Dq [AAV2-hSyn-DIO-hM3D (Gq)-mCherry, 4×10^{12}; University of North Carolina] were injected bilaterally into the mouse ARN. Animals were given carprofen (5 mg/kg body weight, s.c.), anesthetized with 2% isoflurane, and placed in a stereotaxic apparatus. A custom-made bilateral Hamilton syringe apparatus holding two 1-μL Hamilton syringes with 25-gauge needles held 0.9 mm apart was used to perform bilateral injections. Each syringe was filled with 1.0 μL AAV. For the GCaMP6 and ChR2 experiments, mice received a single bilateral injection of AAV 1.2 mm posterior to bregma and 6.0 mm deep. The needles were lowered into place and, after 3 min, 1 μL AAV was injected over 10 min, and the needles were left in situ for a further 10 min before being withdrawn. For the ArchT and eNpHR3.0 experiments, mice received two bilateral injections (1 μL per injection per hemisphere) at 1.0 and 1.2 mm posterior to bregma and 5.7 mm depth. Some mice received bilateral 1-μL coinjections of GCaMP6s and hM3Dq AAVs.

Brain Slice Electrophysiology and Calcium Imaging. Electrophysiological recordings of ARN^{KISS} neurons were carried out as described previously (27). Briefly, coronal brain slices (250 μm thick) were placed under an upright epifluorescence microscope and constantly perfused (1.5 mL/min) with 95% O_2/5% CO_2-equilibrated 30 °C artificial cerebrospinal fluid (aCSF; 120 mM NaCl, 3 mM KCl, 26 mM $NaHCO_3$, 1 mM NaH_2PO_4, 2.5 mM $CaCl_2$, 1.2 mM $MgCl_2$, and 10 mM glucose). Neurons expressing GFP or tdTomato were first visualized by brief fluorescence illumination, and subsequently approached using infrared differential interference contrast optics. ARN^{KISS} neuron action potential firing was recorded in voltage clamp mode using the cell-attached loose patch configuration. Recording electrodes (3 to 5 MΩ) were filled with aCSF including 10 mM Hepes, and low-resistance seals (10 to 30 MΩ) were achieved. Electrophysiological signals were recorded using a MultiClamp 700B amplifier connected to a Digidata 1440A digitizer (Molecular Devices). Signals were low-pass-filtered at 3 kHz before being digitized at a rate of 10 kHz. Signal acquisition was carried out with pClamp 10 (Molecular Devices). Spontaneous spikes were detected using the threshold-crossing method in pClamp 10. Action potential firing was monitored for >2 min before 5-min illumination with a 532-nm laser (0.6 mW; IkeCool) delivered through a fiber optic (200 μm diameter, N.A. 0.37; Doric Lenses) placed above the surface of the slice, near the recorded cell. For chemogenetic experiments, action potential firing of ARN^{KISS} neurons was monitored for >3 min before CNO (1 to 10 μM) was bath-applied for 10 min. Statistical comparisons were undertaken using the nonparametric Friedman tests, with the sample size used in tests being the number of neurons.

Brain slice calcium imaging was carried out as previously reported (41). In brief, brain slices (as above) were illuminated through a 40× immersion objective, using the xenon arc light source (300 W; filtered by a GFP filter cube, excitation 460 to 480 nm; Olympus) and the shutter of a Lambda DG-4 (Sutter Instruments). Epifluorescence (485-nm long pass and emission 495 to 540 nm) was collected using a Hamamatsu ORCA-ER digital CCD camera. A focal plane including several fluorescent ARN^{KISS} somata was chosen and acquisitions (100-ms light exposure at 2 Hz for 10 to 20 min) were started. For analysis, time series of images were processed in ImageJ (NIH). Regions of interest composed of individual in-focus fluorescent ARN^{KISS} somata with average fluorescence intensity were measured in each frame. Fluorescence intensity data were analyzed using scripts written in R (www.r-project.org/) or using pClamp 10. Relative fluorescence changes were calculated using the following formula: $\Delta F/F = (Ft - F)/F \times 100$, where F is the baseline fluorescence intensity calculated as the mean fluorescence intensity over a 2-min period preceding drug applications and Ft is the test fluorescence.

Fiber Photometry. Following AAV injection of GCaMP6s, an optical fiber (400 μm diameter, 0.48 N.A.; Doric Lenses) was positioned immediately above the midcaudal ARN and the mouse then gonadectomized. Mice were housed individually and allowed to recover for at least 3 wk with daily handling and habituation to the fiber photometry recording setup. Over a period of 3 to 10 wk following surgery, fluorescence signals were recorded from freely behaving mice in their home cages. Mice injected with GCaMP6s and hM3Dq AAVs received a single injection of CNO (2 mg/kg, s.c.) during the recording.

Fluorescence signals were acquired using a fiber photometry system based on a previously published design (20). All optical components were purchased from Doric Lenses. Excitation light was provided by violet (referred to as 405-nm) and blue (referred to as 490-nm) fiber-coupled LEDs which were sinusoidally modulated at 531 and 211 Hz, respectively. Each excitation line was passed through an excitation filter (400 to 410 nm and 460 to 490 nm) and focused into a 400-μm optic fiber which connected to the mouse. Emitted fluorescence was collected by the same fiber, passed through a 500- to 550-nm emission filter, and focused onto a photoreceiver (2151; Newport). Two GCaMP6s emission signals were recovered by demodulating the 405-nm (531-Hz) and 490-nm (211-Hz) signals. The 405-nm signal reported the excitation/emission of GCaMP6s at its isosbestic point and was used as a background (non–calcium-dependent) signal. The 490-nm signal reported calcium-dependent GCaMP6s excitation/emission and was used to infer changes in $[Ca^{2+}]i$. The signals were modulated/demodulated and recorded at 10 Hz with custom software (Tussock Innovation). Signals from the 405-nm control channel were subtracted from the 490-nm channel before analysis. Photometry data could either be collected continuously or in 5 s on/15 s off scheduled mode. The power output at the tip of the fiber was set at 50 μW. Fluorescence signals (490 to 405 nm) were collected and converted to $\Delta F/F$ (%) values as follows: $\Delta F/F = 100 \times (F - Fb)/F$, where Fb was the basal fluorescence signal between events and F was the recorded fluorescence.

To assess the relationship of calcium events with pulsatile LH secretion, freely behaving mice were attached to the fiber photometry system and LH secretion was measured by obtaining 3-μL blood samples every 3 to 6 min from the tail tip over a period of 60 to 80 min. Blood sampling and subsequent

ELISA measurement of LH were undertaken as reported previously (12, 23). The assay sensitivity was 0.04 ng/mL, with intra- and interassay coefficients of variation of 9.3 and 10.5%, respectively.

Optogenetic Experiments. Adult control and experimental mice were implanted with indwelling unilateral or bilateral optic fibers (200 μm diameter, pitch 0.9 mm, 0.37 N.A.; Doric Lenses) at the time of AAV injection. Fibers were implanted 1.1 mm posterior to bregma, centered around the sagittal sinus, and 5.7 mm deep. Mice were then habituated for 2 to 5 wk before undergoing the optogenetic activation and bleeding protocol.

For ChR2 optogenetic studies, intact diestrous female and male mice were connected to the laser and 15 min later given 5-ms pulses of blue light (473 nm, 5 mW; DPSS laser; IkeCool) for 1 min at a frequency of 10 Hz, repeated three times over 30-min intervals. Serial 3-μL blood samples were collected from the tail tip at −12, −6, 0, 3, 6, 9, 12, 18, 24, and 30 min, where 0 was the start of the laser stimulation. Statistical analysis of evoked LH values was undertaken using one-way repeated-measures ANOVA with Dunnett's post hoc test, comparing values with the −6-min LH level.

For inhibitory optogenetic experiments, mice GDX at the time of AAV injection were attached to the laser patch cord in their home cages and left to acclimate for 15 min, and 5-min blood sampling (3 μL per sample) was undertaken for 180 min as described above. The laser was turned on for a 30-min period after 90 min of baseline sampling. Illumination with constant green light from a DPSS laser (532 nm, ∼5 mW per fiber; IkeCool) was controlled by a Master9 stimulator. As a control in ArchT experiments, four mice underwent a second bleeding experiment, at least 2 wk after the first, in which they received blue light illumination (472 nm). The frequency and amplitude of pulses were determined for the 0- to 85-min baseline period, the 30-min laser illumination period, and the two 30-min periods thereafter. Taking insight from the fiber photometry results, an LH pulse in GDX mice was defined as a peak level of LH >10% above the preceding value. For each detected pulse, the amplitude was determined by subtracting the highest LH value from the basal value immediately before the onset of the pulse. Data were compared using one-way repeated-measures ANOVA with post hoc Dunnett's tests comparing the baseline with illumination and postillumination time periods.

Immunohistochemistry. Immunofluorescence was undertaken as reported previously (24). Coronal brain sections (30 μm thick) covering the full length of the ARN were used to determine the locations of optic fibers and/or processed for dual-label analysis. Antisera against GFP (1:5,000; Aves Labs) were used to detect GCaMP6. Dual fluorescence images were captured on a Nikon A1+ inverted confocal microscope. Two sections at each of the rostral, middle, and caudal levels of the ARN (Fig. S5) were analyzed in each mouse by counting the total number of cells that expressed τGFP or tdTomato, reporting kisspeptin expression, and either GFP (GCaMP6), tdTomato (ArchT), or eYFP (eNpHR3.0).

ACKNOWLEDGMENTS. The authors thank Mr. Leo van Rens, EMTech, University of Otago, for technical assistance. These studies were supported by the New Zealand Health Research Council, New Zealand Royal Society Marsden Fund, and BBSRC (BB/K003178/1).

1. Le Tissier P, et al. (2017) An updated view of hypothalamic-vascular-pituitary unit function and plasticity. *Nat Rev Endocrinol* 13:257–267.
2. Lightman SL, Conway-Campbell BL (2010) The crucial role of pulsatile activity of the HPA axis for continuous dynamic equilibration. *Nat Rev Neurosci* 11:710–718.
3. Leng G, Brown D (1997) The origins and significance of pulsatility in hormone secretion from the pituitary. *J Neuroendocrinol* 9:493–513.
4. Russell GM, Kalafatakis K, Lightman SL (2015) The importance of biological oscillators for hypothalamic-pituitary-adrenal activity and tissue glucocorticoid response: Coordinating stress and neurobehavioural adaptation. *J Neuroendocrinol* 27:378–388.
5. Dierschke DJ, Bhattacharya AN, Atkinson LE, Knobil E (1970) Circhoral oscillations of plasma LH levels in the ovariectomized rhesus monkey. *Endocrinology* 87:850–853.
6. Belchetz PE, Plant TM, Nakai Y, Keogh EJ, Knobil E (1978) Hypophysial responses to continuous and intermittent delivery of hypopthalamic gonadotropin-releasing hormone. *Science* 202:631–633.
7. Knobil E (1980) The neuroendocrine control of the menstrual cycle. *Recent Prog Horm Res* 36:53–88.
8. Goodman RL, Karsch FJ (1981) The hypothalamic pulse generator: A key determinant of reproductive cycles in sheep. *Biological Clocks in Seasonal Reproductive Cycles*, eds Follett BK, Follett DE (John Wright & Sons, Bristol, England), Vol 32, pp 223–236.
9. Seminara SB, et al. (2003) The GPR54 gene as a regulator of puberty. *N Engl J Med* 349:1614–1627.
10. de Roux N, et al. (2003) Hypogonadotropic hypogonadism due to loss of function of the KiSS1-derived peptide receptor GPR54. *Proc Natl Acad Sci USA* 100:10972–10976.
11. Kirilov M, et al. (2013) Dependence of fertility on kisspeptin-Gpr54 signaling at the GnRH neuron. *Nat Commun* 4:2492.
12. Steyn FJ, et al. (2013) Development of a methodology for and assessment of pulsatile luteinizing hormone secretion in juvenile and adult male mice. *Endocrinology* 154: 4939–4945.
13. Uenoyama Y, et al. (2015) Lack of pulse and surge modes and glutamatergic stimulation of luteinising hormone release in Kiss1 knockout rats. *J Neuroendocrinol* 27:187–197.
14. Herbison AE (2016) Control of puberty onset and fertility by gonadotropin-releasing hormone neurons. *Nat Rev Endocrinol* 12:452–466.
15. Lehman MN, Coolen LM, Goodman RL (2010) Minireview: Kisspeptin/neurokinin B/dynorphin (KNDy) cells of the arcuate nucleus: A central node in the control of gonadotropin-releasing hormone secretion. *Endocrinology* 151:3479–3489.
16. Navarro VM, et al. (2009) Regulation of gonadotropin-releasing hormone secretion by kisspeptin/dynorphin/neurokinin B neurons in the arcuate nucleus of the mouse. *J Neurosci* 29:11859–11866.
17. de Croft S, Boehm U, Herbison AE (2013) Neurokinin B activates arcuate kisspeptin neurons through multiple tachykinin receptors in the male mouse. *Endocrinology* 154:2750–2760.
18. Qiu J, et al. (2016) High-frequency stimulation-induced peptide release synchronizes arcuate kisspeptin neurons and excites GnRH neurons. *Elife* 5:e16246.
19. Wakabayashi Y, et al. (2010) Neurokinin B and dynorphin A in kisspeptin neurons of the arcuate nucleus participate in generation of periodic oscillation of neural activity driving pulsatile gonadotropin-releasing hormone secretion in the goat. *J Neurosci* 30:3124–3132.
20. Lerner TN, et al. (2015) Intact-brain analyses reveal distinct information carried by SNc dopamine subcircuits. *Cell* 162:635–647.
21. Yeo SH, et al. (October 28, 2016) Visualisation of Kiss1 neurone distribution using a Kiss1-CRE transgenic mouse. *J Neuroendocrinol*, 10.1111/jne.12435.
22. Alexander GM, et al. (2009) Remote control of neuronal activity in transgenic mice expressing evolved G protein-coupled receptors. *Neuron* 63:27–39.
23. Czieselsky K, et al. (2016) Pulse and surge profiles of luteinizing hormone secretion in the mouse. *Endocrinology* 157:4794–4802.
24. Han SY, McLennan T, Czieselsky K, Herbison AE (2015) Selective optogenetic activation of arcuate kisspeptin neurons generates pulsatile luteinizing hormone secretion. *Proc Natl Acad Sci USA* 112:13109–13114.
25. Chow BY, et al. (2010) High-performance genetically targetable optical neural silencing by light-driven proton pumps. *Nature* 463:98–102.
26. Mattis J, et al. (2011) Principles for applying optogenetic tools derived from direct comparative analysis of microbial opsins. *Nat Methods* 9:159–172.
27. de Croft S, et al. (2012) Spontaneous kisspeptin neuron firing in the adult mouse reveals marked sex and brain region differences but no support for a direct role in negative feedback. *Endocrinology* 153:5384–5393.
28. Herbison AE (2015) Physiology of the adult GnRH neuronal network. *Knobil and Neill's Physiology of Reproduction*, eds Plant TM, Zeleznik AJ (Academic, San Diego), 4th Ed, Vol 1, pp 399–467.
29. Sternson SM, Eiselt AK (2017) Three pillars for the neural control of appetite. *Annu Rev Physiol* 79:401–423.
30. Fu LY, van den Pol AN (2010) Kisspeptin directly excites anorexigenic proopiomelanocortin neurons but inhibits orexigenic neuropeptide Y cells by an indirect synaptic mechanism. *J Neurosci* 30:10205–10219.
31. Hu MH, et al. (2015) Relative importance of the arcuate and anteroventral periventricular kisspeptin neurons in control of puberty and reproductive function in female rats. *Endocrinology* 156:2619–2631.
32. Lehman MN, Hileman SM, Goodman RL (2013) Neuroanatomy of the kisspeptin signaling system in mammals: Comparative and developmental aspects. *Adv Exp Med Biol* 784:27–62.
33. Raimondo JV, Kay L, Ellender TJ, Akerman CJ (2012) Optogenetic silencing strategies differ in their effects on inhibitory synaptic transmission. *Nat Neurosci* 15:1102–1104.
34. Yip SH, Boehm U, Herbison AE, Campbell RE (2015) Conditional viral tract tracing delineates the projections of the distinct kisspeptin neuron populations to gonadotropin-releasing hormone (GnRH) neurons in the mouse. *Endocrinology* 156:2582–2594.
35. Herde MK, Iremonger KJ, Constantin S, Herbison AE (2013) GnRH neurons elaborate a long-range projection with shared axonal and dendritic functions. *J Neurosci* 33: 12689–12697.
36. Iremonger KJ, Porteous R, Herbison AE (2017) Spike and neuropeptide-dependent mechanisms control GnRH neuron nerve terminal Ca^{2+} over diverse time scales. *J Neurosci* 37:3342–3351.
37. Glanowska KM, Moenter SM (2015) Differential regulation of GnRH secretion in the preoptic area (POA) and the median eminence (ME) in male mice. *Endocrinology* 156: 231–241.
38. Ramaswamy S, Guerriero KA, Gibbs RB, Plant TM (2008) Structural interactions between kisspeptin and GnRH neurons in the mediobasal hypothalamus of the male rhesus monkey (*Macaca mulatta*) as revealed by double immunofluorescence and confocal microscopy. *Endocrinology* 149:4387–4395.
39. Keen KL, Wegner FH, Bloom SR, Ghatei MA, Terasawa E (2008) An increase in kisspeptin-54 release occurs with the pubertal increase in luteinizing hormone-releasing hormone-1 release in the stalk-median eminence of female rhesus monkeys in vivo. *Endocrinology* 149:4151–4157.
40. Ainsworth M, et al. (2012) Rates and rhythms: A synergistic view of frequency and temporal coding in neuronal networks. *Neuron* 75:572–583.
41. Piet R, Fraissenon A, Boehm U, Herbison AE (2015) Estrogen permits vasopressin signaling in preoptic kisspeptin neurons in the female mouse. *J Neurosci* 35: 6881–6892.